Eur. Phys. J. C (2019) 79:1014
https://doi.org/10.1140/epjc/s10052-019-7511-z

THE EUROPEAN PHYSICAL JOURNAL C

Regular Article - Theoretical Physics

Quantum charged spinning massless particles in 2 + 1 dimensions

Ivan Morales[1,a], **Bruno Neves**[1,2,b], **Zui Oporto**[1,3,c], **Olivier Piguet**[1,4,d]

[1] Departamento de Física, Universidade Federal de Viçosa (UFV), Viçosa, MG, Brazil
[2] Department of Astrophysics, Cosmology and Fundamental Interactions, Brasilian Center for Research in Physics, CBPF, Rio de Janeiro 22290-180, Brazil
[3] Carrera de Física, Universidad Mayor de San Andrés, La Paz, Bolivia
[4] Present address: Praça Graccho Cardoso, 76/504, Aracaju, SE 45015-180, Brazil

Received: 15 October 2019 / Accepted: 23 November 2019 / Published online: 16 December 2019

Abstract Motivated by the conduction properties of graphene discovered and studied in the last decades, we consider the quantum dynamics of a massless, charged, spin 1/2 relativistic particle in three dimensional space-time, in the presence of an electrostatic field in various configurations such as step or barrier potentials and generalizations of them. The field is taken as parallel to the y coordinate axis and vanishing outside of a band parallel to the x axis. The classical theory is reviewed, together with its canonical quantization leading to the Dirac equation for a 2-component spinor. Stationary solutions are numerically found for each of the field configurations considered, from which we calculate the mean quantum trajectories of the particle and compare them with the corresponding classical trajectories, the latter showing a classical version of the Klein phenomenon. Transmission and reflection probabilities are also calculated, confirming the Klein phenomenon.

Contents

1 Introduction . . . 1
2 Canonical analysis and quantization . . . 4
2.1 Action and classical equations of motion . . . 4
2.2 Canonical analysis . . . 5
2.2.1 Analysis of the constraints . . . 5
2.2.2 Gauge invariances . . . 6
2.3 Quantization . . . 6
3 The quantum relativistic massless particle in an electrostatic potential . . . 6
3.1 General setting . . . 6
3.1.1 Asymptotic states . . . 7
3.1.2 Scattering boundary conditions . . . 8
3.1.3 Reflection and transmission coefficients . . . 8
3.1.4 Comparison with the classical motion . . . 9
3.2 Some examples . . . 9
3.2.1 Square step potential . . . 9
3.2.2 Square barrier potential . . . 10
3.2.3 Oblique step potential . . . 11
3.2.4 Approximatively constant electric field . . . 13
3.2.5 Oblique barrier potential . . . 14
3.2.6 Oblique well potential . . . 15
4 Conclusions . . . 15
Appendices . . . 16
A Notations and conventions . . . 16
B Classical equations in the case of a y-dependent electrostatic field . . . 16
References . . . 17

[a] e-mail: mblivan@gmail.com
[b] e-mail: bruno.lqg@gmail.com
[c] e-mail: azurnasirpal@gmail.com
[d] e-mail: opiguet@yahoo.com

1 Introduction

By the end of 1928, the same year that Dirac published its "quantum theory of the electron" paper, Klein [1,2] analysed the behaviour of quantum relativistic electrons in presence of a step barrier potential. His calculations revealed that, for a sufficiently high enough energy barrier, electrons can push forward against it and trespassing to the classical forbidden region by switching the sign of their kinetic energy, the latter a by-product of the Dirac Hamiltonian having negative energy states in its spectrum. This theoretical prediction is the so-called Klein phenomenon or Klein tunnelling, characterized by the absence of the typical exponential suppression found in non-relativistic quantum mechanics.

During the analysis of the transmission and reflection coefficients, Klein apparently also found on a first approach that more electrons were scattered back by the potential when

compared with the number of incident ones. This implied a reflection coefficient greater than one and in consequence a negative transmission coefficient. But thanks to an insightful observation by Pauli, as Klein himself acknowledged, this situation was resolved by noticing that inside the barrier potential the momentum changes its direction, being here opposite to its group velocity. The modification suffices to restore the physical meaning of the reflection and transmission coefficients. It has to be mentioned that although Klein never considered this last result a real paradox – and in fact that word does not appear in his paper – this phenomenon is many times still known as the "Klein paradox". A very interesting historical approach to the Klein gedanken experiment can be seen in [2–5].

It is by now widely understood [2] that this phenomenon is a pure relativistic effect. In the regions where the total energy E is smaller than the critical value $V(\mathbf{x})-mc^2$, i.e., where the kinetic energy is negative, the particle still propagates, with an oscillating wave function. In a solid state context, this can be interpreted as a particle (an electron) propagating in the valence band, whereas in the region where the potential is such that the kinetic energy is positive, $E > V(\mathbf{x})+mc^2$, one has a particle propagating in the conduction band. We shall refer to such situations as the propagation of a VB, respectively CB, particle (see Figure 2 in [2]). Thus a relativistic particle may go through a potential step or barrier without exponential damping irrespective of the energy value, provided $|E-V| > mc^2$, in contrast to the non-relativistic case. The classical counterpart of this effect is that the potential is repulsive or attractive depending on the sign of the kinetic energy (see Appendix B).

By the time Klein published his work, it was conjectured that the "paradoxical" result mentioned above was caused by the abrupt discontinuity of the step potential. Could a smoother potential get rid of this unintuitive result? In this respect, it was shown by Sauter [6] , that the conjecture was partially correct: for weak smooth fields the reflection and transmission coefficients behaves as expected, but for strong fields Klein phenomenon shows up despite of the potential being continuous.

Later, Hund [7] reconsidered the analysis from the quite different perspective of multiparticle theory in quantum field theory. Although his calculations were limited to the Klein-Gordon equation, it was clear by the time that the potential barrier was spontaneously producing pairs of charged particles/antiparticles. The analysis for the Dirac field was successfully accomplished fifty years later by Nikishov [8–10]). Since then, the Klein phenomenon has been adopted by some authors as a good and pedagogical starting point to justify the introduction of the multi-particle picture of the Dirac equation against the single particle stand point. A closer examination of the Klein phenomenon shows that this is not necessarily true, since Klein tunnelling can occur even when the potential is not high enough to produce pairs [2]. It has also been suggested to trace Klein tunnelling back to the classical relativistic theory [11,12] where massless charged particles possess a very special dynamics in the presence of external electromagnetic fields. Let us mention in particular a result implicit in [11–13] that for a spinless particle travelling with velocity $\mathbf{v} = (0, v_{0y} = c, 0)$ right towards a constant electric field $(0, E, 0)$ barrier, no matter its intensity, the particle experience no back scattering at all (see equation (24) of [13]). The explanation of this unexpected result is clear if we remember that the massless and spinless particle already moves at the speed of light; a reflection would imply a turning point at which the velocity would be zero, which is not admissible. Therefore there is no such classically forbidden region for this particular case. The reader can refer to [12] for further discussions on this point.

It has to be noted that Klein phenomenon (along with the *Zitterbewegung*) remains as a theoretical prediction with no experimental evidence so far in high energy physics. This fact seems to have contributed to keep alive the debate almost a century after Klein's work.[1] A more refreshing debate about the Klein phenomenon has been gaining attention in recent years, this time in the context of condensed matter physics, more specifically the physics of graphene (see [14] for a review). Indeed, the band structure of the monolayer of carbon known as graphene has been demonstrated to be a suitable testing ground for quantum electrodynamics phenomena. Its effective charge carriers obey a relativistic linear energy-momentum dispersion relation of the form $E = v_{\mathrm{F}}|\mathbf{p}|$, the Fermi critical velocity $v_{\mathrm{F}} \approx 1000$ km/s playing the role of the "light velocity" c. Thus, graphene stands out as an exceptional material for testing such a special quantum behaviour. In particular, Klein tunnelling has being experimentally confirmed ten years ago [3,15]. More generally, a number of devices for applications have been proposed in order to investigate this phenomenon [3,16].

The significant advances in the physics of graphene, first on Klein tunnelling [17–19], then on the quantum Hall effect [20,21], on the scattering properties and "electronic optics" [22–26] and also some recent results on the so-called topological semi-metals, e.g. Weyl semi-metals [27,28], are promising for novel applications for fundamental physics as well as for probing for new theoretical and experimental electronic, optical and mechanical properties. On the other hand, the novelties of graphene from the theoretical point of view has not been unnoticed for the quantum gravity community [29–36], once again offering a unique opportunity to develop future experiments to guide theory.

[1] An inspection of the cross reference database on the inspirehep.net web site reveals a significant increasing of citations to the original Klein article since 2010 (http://inspirehep.net/record/48390/citations).

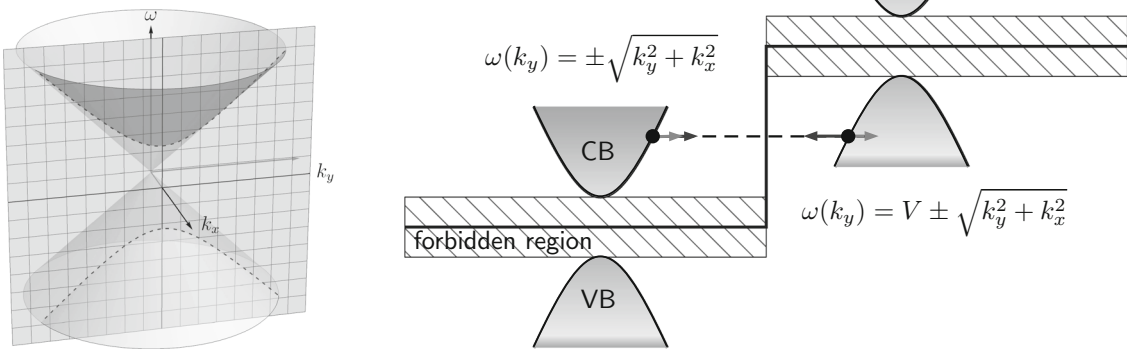

(a) The figure shows the dispersion relation for massless particles in 2+1 dimensions (the double conic surface). For k_x fixed, the particle is constrained to move along the hyperbola (dashed curve) that lies in the plane k_x = const.; in this case the effective dispersion relation is $\omega(k_y) = \pm\sqrt{k_y^2 + k_x^2}$, which is equivalent to the dispersion relation of a particle of mass $|k_x|$ in natural units.

(b) Representation of the transmission of a relativistic massless particle through a square potential barrier step of height V. For an oblique collision the effective dispersion relation corresponds to a hyperbola. The dashed regions are the forbidden ones and separate the positive kinetic energy states (CB particles) from the negative ones (VB particles). For CB particles the momentum (long vector) points in the same direction as that of the velocity (short vector); for VB particles the momentum and the velocity point in opposite directions. For a frontal collision the hyperbola would degenerate in cone and there would be no forbidden regions. See [2,37]

Fig. 1 Massles particle kinematics

Within the theoretical framework of condensed matter physics Klein tunnelling can be interpreted as the interband tunnelling (i.e. the transition of an electron from the conduction band to the valence band). The interband transition is possible because the presence of the step barrier modifies the dispersion relation to the right of the step (see [2,37] and Fig. 1b). The electrons in the conduction band are analogous of the ordinary electrons with positive energies in relativistic quantum mechanics, with its velocity and momentum pointing in the same direction. The electrons in the valence band are analogous to negative energy electrons; in this case the velocity and momentum points to opposite directions. A similar description applies to holes (the absence of an electron in any of the bands). Holes in the conduction band are the equivalent to positive energy positrons, with the velocity and momentum pointing to the same direction (the difference with electrons would be in the direction of the current because of the sign of the charge) whereas holes in the valence band corresponds to negative energy positrons. This is a framework compatible with the single particle picture of the Dirac equation. It is clear that the problem of charge conservation has no place in this case. What is most remarkable is that this description already contains the clue ingredient pointed out almost 100 years ago by Klein and Pauli, i.e., electrons inside the barrier has negative kinetic energies, and its momentum experiences a change of sign with respect to the group velocity.

The existence of such peculiar properties justifies further theoretical investigations through a formalism based on fundamental principles, namely, from a Lagrangian point of view and following the Dirac-Bergmann prescription to implement the canonical quantization. A complete quantum analysis for a spinning, charged and massless particle in $(2 + 1)$ dimensions is still missing, although many results may be found in the literature.

For effectively massless fermions such as in graphene, there is no energy gap, thus the Klein tunnelling, occurs as soon as the energy E is lower than the potential for direct incident electrons. For oblique incident ones the component of the momentum parallel to the potential barrier emulates, in some respects, an effective non zero mass, and thus a non zero gap separating the negative and positive kinetic energy states reappears, as our calculations will confirm (see Fig. 1a below).

We must stress that, motivated by the dynamics of electrons in materials such as graphene, we deal here with a spin 1/2 massless particle obeying a Dirac equation, which may be obtained by a quantization procedure from a supersymmetric classical theory involving Grassmann variables whose quantum operator version is represented by Dirac matrices. This

must be contrasted with the so-called anyon theories [38–40][2] – also in 3D space-time – where the classical theory has only ordinary variables and the quantum wave equation is not of the Dirac form. There, spin can take arbitrary values. Moreover, at least in the references [38–40], the mass is different from zero.

The aim of the present paper is to discuss the quantum dynamics of a relativistic massless charged fermions in (2+1) dimensional space-time, in the context of Dirac wave mechanics. We shall follow a strictly quantum-mechanical approach [1,2,4–6,12,17,18,37,41–43], and not the full quantum field theoretic one [7–11,44–46] which would take into account processes such as pair production and the possibility of e^-e^- bound states [46].

We begin in Sect. 2 with the full canonical quantization of the theory, whose classical aspects have been studied in a previous work [13]. Therefore, we start with the analysis of the constraints for the spinning charged particle, taken as massive. We follow then the Dirac-Bergmann prescription for the quantization in the massless case.

In Sect. 3 we start the study of the quantum massless particle coupled with an external electrostatic potential. A technical analysis of the boundary conditions is described in order to make basic points more transparent and we present the results for various types of potentials, square or more general ones. When necessary, comparisons with the literature [2–5,14,41–43] – which mainly deals with square potentials – will be made. In each case we calculate the reflection and transmission probabilities, and we compare the quantum mean trajectory of the particle with its classical counterpart, as a check of the correspondence principle. We observe the quantum effect *Zitterbewegung*, i.e., a jittery motion of the mean trajectory due to the superposition of the right and left moving waves – when both are present. Two appendices are dedicated to the definition of conventions and to the classical equations of motion in a special case of interest.

Computations in concrete cases are done with the help of the software Mathematica [47]. Interested readers may download (and use) the computer program from the arXiv site at the link https://arxiv.org/src/1910.03059v2/anc/Trajectories.nb and save it as a file: Trajectories.nb.

2 Canonical analysis and quantization

2.1 Action and classical equations of motion

The classical motion of a relativistic spinning particle of mass[3] m and electric charge q in the presence of an external electromagnetic field $A_\mu(x)$ reads, in covariant form:

$$S = \int_{\mathcal{C}} d\lambda\, L(X(\lambda), \dot{X}(\lambda)), \tag{2.1}$$

where $\mathcal{C}$ is a path in dimension 3 spacetime[4] parametrized by λ. X represents the generalized coordinates x^μ, e, ψ^μ, χ, ψ_5, the last three ones being odd (anticommuting) Grassmann numbers which describe the classical spin degree of freedom. Dot above the variables denotes derivatives with respect to λ. The Lagrangian is given by [13,48–50]

$$\begin{aligned} L(X,\dot{X}) = &-\frac{1}{2}\left(\frac{\dot{x}^\mu}{e}\left(\dot{x}_\mu - i\chi\psi_\mu\right) - i\psi^\mu\dot{\psi}_\mu\right) \\ &-\frac{1}{2}\left(em^2 + i\left(\psi_5\dot{\psi}_5 + m\chi\psi_5\right)\right) \\ &-\left(qA_\mu(x)\dot{x}^\mu + \frac{iq}{2}e\psi^\mu F_{\mu\nu}(x)\psi^\nu\right), \end{aligned} \tag{2.2}$$

A_μ being the electromagnetic 3-potential and $F_{\mu\nu} = \partial_\mu A_\nu - \partial_\nu A_\mu$ the electromagnetic tensor field. The odd Grassmann variable ψ_5 may be ommitted in the massless case $m = 0$.

The action is invariant, up to boundary terms, under two gauge symmetries. The first one is its invariance under the λ–reparametrizations:

$$\begin{aligned} &\delta^{\mathrm{R}}_\varepsilon x^\mu = \varepsilon\dot{x}^\mu, \quad \delta^{\mathrm{R}}_\varepsilon\psi^\mu = \varepsilon\dot{\psi}^\mu, \quad \delta^{\mathrm{R}}_\varepsilon\psi_5 = \varepsilon\dot{\psi}_5, \\ &\delta^{\mathrm{R}}_\varepsilon e = \dot{\varepsilon}e + \varepsilon\dot{e}, \quad \delta^{\mathrm{R}}_\varepsilon\chi = \dot{\varepsilon}\chi + \varepsilon\dot{\chi}, \end{aligned} \tag{2.3}$$

where $\varepsilon(\lambda)$ is an infinitesimal parameter. The second gauge invariance is a supersymmetry:

$$\begin{aligned} &\delta^{\mathrm{S}}_\alpha x^\mu = i\alpha\psi^\mu, \quad \delta^{\mathrm{S}}_\alpha\psi^\mu = \alpha\frac{1}{e}\left(\dot{x}^\mu - \frac{i}{2}\chi\psi^\mu\right), \\ &\delta^{\mathrm{S}}_\alpha\psi_5 = m\alpha + \frac{i}{me}\alpha\psi_5\left(\dot{\psi}_5 - \frac{m\chi}{2}\right), \\ &\delta^{\mathrm{S}}_\alpha e = i\alpha\chi, \quad \delta^{\mathrm{S}}_\alpha\chi = 2\dot{\alpha}, \end{aligned} \tag{2.4}$$

where $\alpha(\lambda)$ is an odd infinitesimal parameter. The electromagnetic potential and field accordingly transform as

$$\begin{aligned} &\delta^{\mathrm{R}}_\varepsilon A_\mu = \varepsilon\dot{A}_\mu, \quad \delta^{\mathrm{R}}_\varepsilon F_{\mu\nu} = \varepsilon\dot{F}_{\mu\nu} \\ &\delta^{\mathrm{S}}_\alpha A_\mu = i\alpha\partial_\rho A_\mu\psi^\rho, \quad \delta^{\mathrm{S}}_\alpha F_{\mu\nu} = i\alpha\partial_\rho F_{\mu\nu}\psi^\rho \end{aligned}$$

A superalgebra structure is evidenced by the commutation rules

$$\begin{aligned} &\left[\delta^{\mathrm{R}}_{\varepsilon_1}, \delta^{\mathrm{R}}_{\varepsilon_2}\right] = \delta^{\mathrm{R}}_{\varepsilon_2\dot{\varepsilon}_1 - \varepsilon_1\dot{\varepsilon}_2}, \quad \left[\delta^{\mathrm{R}}_\varepsilon, \delta^{\mathrm{S}}_\alpha\right] = \delta^{\mathrm{S}}_{-\varepsilon\dot{\alpha}}, \\ &\left[\delta^{\mathrm{S}}_{\alpha_1}, \delta^{\mathrm{S}}_{\alpha_2}\right] = \delta^{\mathrm{R}}_{\tilde{\varepsilon}} + \delta^{\mathrm{S}}_{\tilde{\alpha}}, \end{aligned}$$

where $\tilde{\varepsilon} = 2i\alpha_2\alpha_1/e$ and $\tilde{\alpha} = -i\alpha_2\alpha_1\chi/e$. Note that the structure "constant" in the last commutator depends on the variable χ.

The equations of motion obtained by the variation of the action (2.1) read

[2] We thank Dr. Subir Gosh for appointing these references to us.

[3] We will be most interested in the massless particle, but in this section we consider the massive case for the sake of generalization.

[4] The spacetime index μ takes the values 0, 1, 2, the metric is $\eta_{\mu\nu} = \mathrm{diag}(1,-1,-1)$. We use natural units with $c = \hbar = 1$ (c would be the Fermi velocity in applications such as graphene physics).

$$
\begin{aligned}
&\frac{\mathrm{d}}{d\lambda}\left(\frac{\dot{x}_\mu}{e}-i\frac{\chi\psi_\mu}{2e}\right)\\
&\quad -q\left(F_{\mu\nu}\dot{x}^\nu+\frac{i}{2}e\psi^\rho\partial_\mu F_{\rho\sigma}\psi^\sigma\right)=0,\\
&\frac{1}{2}\left(\frac{\dot{x}_\mu\dot{x}^\mu}{e^2}-i\frac{\chi\dot{x}_\mu\psi^\mu}{e^2}+iq\psi^\mu F_{\mu\nu}\psi^\nu\right)-\frac{m^2}{2}=0,\\
&i\left(\dot{\psi}_\mu-\frac{\dot{x}_\mu\chi}{2e}-qeF_{\mu\nu}\psi^\nu\right)=0,\\
&\quad -i\left(\dot{\psi}_5-\frac{m}{2}\chi\right)=0,\\
&\frac{i}{2}\left(\frac{\dot{x}^\mu\psi_\mu}{e}-m\psi_5\right)=0.
\end{aligned}
\tag{2.5}
$$

Note that we could choose $\chi=0$ as a gauge fixing condition, which leaves a residual supersymmetry (2.4) with a constant parameter α, which in turn could be fixed, in the massive case, by the condition $\psi_5=0$. This can easily be checked by examining the supersymmetry transformations (2.4) and observing that the fourth of the Eq. (2.5) implies $\dot{\psi}_5=0$ if $\chi=0$.

We display in Appendix B the field equations for the massless charged spinning particle in the presence of an electrostatic field depending only on the y coordinate, which is the case of interest in the application part of the paper.

2.2 Canonical analysis

As a preparation for the quantization of the theory we perform a canonical analysis following Dirac's algorithm for systems with constraints [51–54]. We keep a non-zero mass in the present section.

2.2.1 Analysis of the constraints

The conjugate momenta are read out from the Lagrangian (2.2):

$$
\begin{aligned}
&p_\mu=\frac{\partial L}{\partial\dot{x}^\mu}=-\frac{\dot{x}_\mu}{e}-qA_\mu+\frac{i\chi\psi_\mu}{2e},\\
&p_e=\frac{\partial L}{\partial\dot{e}^\mu}=0,\\
&\mathbb{P}_\mu=\frac{\partial L}{\partial\dot{\psi}^\mu}=-\frac{i\psi_\mu}{2},\qquad p_\chi=\frac{\partial L}{\partial\dot{\chi}}=0,\\
&p_5=\frac{\partial L}{\partial\dot{\psi}^\mu}=\frac{i\psi_5}{2}.
\end{aligned}
\tag{2.6}
$$

Four of these equations relate momenta and generalized coordinates, which means that we have four primary constraints:

$$
\begin{aligned}
&\phi_e=p_e\approx0,\quad \phi_\chi=p_\chi\approx0,\quad \phi_\mu=\mathbb{P}_\mu+\frac{i\psi_\mu}{2}\approx0,\\
&\phi_5=p_5-\frac{i\psi_5}{2}\approx0,
\end{aligned}
\tag{2.7}
$$

where the symbol $\approx$ means a "weak equality", i.e., an equality which will be turned effective only after all the Poisson bracket algebra manipulations are done.

The basic non-vanishing Poisson brackets between the generalized coordinates and their conjugate momenta are given by:

$$
\begin{aligned}
&\{x^\mu,p_\nu\}=\delta^\mu_\nu,\quad \{e,p_e\}=1,\\
&\{\psi^\mu,\mathbb{P}_\nu\}=-\delta^\mu_\nu,\quad \{\chi,p_\chi\}=-1,\quad \{\psi_5,p_5\}=-1.
\end{aligned}
\tag{2.8}
$$

These brackets are "graduated", i.e., they are symmetric if both arguments are Grassmann odd, and antisymmetric otherwise.

Through a Legendre transformation we obtain the canonical Hamiltonian

$$
H_{\mathrm{C}}=-\frac{e}{2}\phi_{\mathrm{KG}}+\frac{i\chi}{2}\phi_{\mathrm{D}}
\tag{2.9}
$$

where

$$
\phi_{\mathrm{KG}}=\Pi^\mu\Pi_\mu-m^2-iq\psi^\mu F_{\mu\nu}\psi^\nu,\qquad \phi_{\mathrm{D}}=\psi_\mu\Pi^\mu+m\psi_5,
\tag{2.10}
$$

with

$$
\Pi_\mu=p_\mu+qA_\mu=-\frac{\dot{x}_\mu}{e}+\frac{i\chi\psi_\mu}{2e}.
$$

Both terms of the canonical Hamiltonian turn out to be secondary constraints assuring the stability of the primary constraints ϕ_e and ϕ_χ:

$$
\phi_{\mathrm{KG}}\approx0,\qquad \phi_{\mathrm{D}}\approx0.
\tag{2.11}
$$

One first notices that the last two constraints in (2.7) have Poisson brackets which do not weakly vanish:

$$
\{\phi_\mu,\phi_\nu\}=-i\eta_{\mu\nu},\quad \{\phi_5,\phi_5\}=i,\quad \{\phi_\mu,\phi_5\}=0,
\tag{2.12}
$$

which means that they are second class. These Poisson brackets form a non-singular 4×4 matrix C_{AB}, with $A=\mu,5$ and $B=\nu,5$:

$$
C_{AB}=\begin{pmatrix}-i\eta_{\mu\nu} & 0\\ 0 & i\end{pmatrix}.
\tag{2.13}
$$

Elimination of the second class constraints ϕ_A is performed by introducing the Dirac brackets

$$
\{U,V\}_{\mathrm{D}}=\{U,V\}-\sum_{A,B}\{U,\phi_A\}\left(C^{-1}\right)^{AB}\{\phi_B,V\},
\tag{2.14}
$$

for any phase space functions U and V. The Dirac brackets of the second class constraints with any phase space function being strongly vanishing, this allows one to solve them right now:

$$\mathbb{P}_\mu = -\frac{i}{2}\psi_\mu, \quad p_5 = \frac{i}{2}\psi_5. \tag{2.15}$$

Phase space is thus reduced, its coordinates being now x^μ, p_μ, ψ_μ, e, p_e, χ, p_χ and ψ_5. The fundamental non-zero Dirac brackets for our system are then given by:

$$\begin{aligned} &\{x^\mu, p_\nu\}_{\mathrm{D}} = \delta^\mu_\nu, \quad \{e, p_e\}_{\mathrm{D}} \quad = 1, \\ &\{\psi_\mu, \psi_\nu\}_{\mathrm{D}} = -i\eta_{\mu\nu}, \quad \{\chi, p_\chi\}_{\mathrm{D}} = -1, \quad \{\psi_5, \psi_5\}_{\mathrm{D}} = i. \end{aligned} \tag{2.16}$$

Finally one checks that the Poisson brackets between the constraints (2.11), the first two of (2.7) and the Hamiltonian (2.9) are weakly zero, i.e., they are either zero or a linear combination of constraints. This means that they are "first class". In particular they are left stable during their evolution with respect to the "time" λ, generated by their brackets with the Hamiltonian. Thus, no new constraint occurs: the present set of constraints is complete.

2.2.2 Gauge invariances

Each first class constraint ϕ_A ($A = \mathrm{KG},\ \mathrm{D},\ e,\ \chi$) generates an invariance under a gauge transformation which, infinitesimally, takes the form

$$\delta_A U = \varepsilon\{U, \phi_A\}_{\mathrm{D}}, \tag{2.17}$$

for any function U of the reduced phase space, with ε an infinitesimal parameter. We see from (2.7), that ϕ_e and ϕ_χ generate arbitrary translations of the coordinates e and χ, respectively. This implies that we can gauge fix each of them to an arbitrary function. We can then read the coefficients e and χ in the canonical Hamiltonian (2.9) as Lagrange multipliers for the constraints ϕ_{KG} and ϕ_{D}, and forget the constraints p_e and p_χ.

We are left with a reduced phase space of coordinates x^μ, p_μ, ψ_μ and ψ_5 and two gauge invariances generated by ϕ_{KG} and ϕ_{D}, obeying the Dirac bracket algebra

$$\{\phi_{\mathrm{D}}, \phi_{\mathrm{D}}\}_{\mathrm{D}} = -i\phi_{\mathrm{KG}}, \tag{2.18}$$

the other brackets being vanishing. They generate the gauge transformations, according to (2.17):

$$\begin{aligned} &\delta_{\mathrm{KG}}\, x^\mu = -\frac{2\varepsilon}{e}\dot{x}^\mu, \quad \delta_{\mathrm{KG}}\, \psi^\mu = -2\varepsilon q F^\mu{}_\nu \psi^\nu, \quad \delta_{\mathrm{KG}}\, \psi_5 = 0 \\ &\delta_{\mathrm{D}}\, x^\mu = \alpha\psi^\mu, \qquad \delta_{\mathrm{D}}\, \psi^\mu = -i\alpha\dot{x}^\mu, \qquad\quad \delta_{\mathrm{D}}\, \psi_5 = i\alpha m \end{aligned} \tag{2.19}$$

2.3 Quantization

From now on we consider the massless case $m = 0$ and therefore one can take $\psi_5 = 0$.

To convert the classical theory to its quantum version, we proceed according to the Dirac scheme [51], promoting the classical expressions A to operators $\hat{A}$, and then impose (anti-)commutation relations on these operators. These (anti-)commutation relations may be viewed as the outcome of the substitution of the Dirac bracket $\{A, B\}_{\mathrm{D}}$ defined in the preceding section by the graded commutator $(i\hbar)^{-1}[\hat{A}, \hat{B}]$. In particular, from (2.16), we find the basic (anti-)commutation relations between the canonical variables:

$$[\hat{x}^\nu, \hat{p}_\mu] = i\hbar\delta^\nu_\mu, \quad [\hat{\psi}_\mu, \hat{\psi}_\nu] = \hbar\eta_{\mu\nu}, \tag{2.20}$$

In a wave mechanics representation, the state is described by a 2-components[5] spinor $\Psi(x)$, and the basic operators are defined as

$$\hat{x}^\mu = x^\mu, \quad \hat{p}_\mu = -i\partial_\mu, \quad \hat{\psi}^\mu = \gamma^\mu/\sqrt{2},$$

where the γ^μ are the 2-dimensional Dirac matrices, with $\gamma^\mu\gamma^\nu + \gamma^\nu\gamma^\mu = 2\eta^{\mu\nu}$.

With this prescription, the first class constraint ϕ_D defined in (2.10) with $m = 0$, yields the Dirac wave equation:

$$\hat{\phi}_D\Psi(x) = \gamma^\mu\left(-i\partial_\mu + qA_\mu\right)\Psi(x) = 0. \tag{2.21}$$

3 The quantum relativistic massless particle in an electrostatic potential

3.1 General setting

We consider the Dirac equation (2.21) for a massless spin 1/2 particle of unit charge $q = 1$ in a static electric field[6] $\mathbf{E} = -\nabla V$, $V(\mathbf{x}) = A_0(\mathbf{x})$ being the electric potential. It reads

$$\left(\gamma^0\left(i\frac{\partial}{\partial t} - V(\mathbf{x})\right) + i\,\gamma^i\frac{\partial}{\partial x^i}\right)\Psi(t, \mathbf{x}) = 0. \tag{3.1}$$

The Dirac Hamiltonian operator is given by

$$H_{\mathrm{D}} = -i\alpha^i\frac{\partial}{\partial x^i} + V(\mathbf{x}). \tag{3.2}$$

The matrices γ^μ and α^i are given in Appendix A.

[5] The present quantization procedure with 2-components spinors holds for the massless case. In the massive case there would be 4 Dirac matrices obeying a Clifford algebra, corresponding to the 4 odd variables ψ_μ, ψ_5; the dimension of the representation of this algebra would thus been at least 4.

[6] See Appendix A for our notations and conventions.

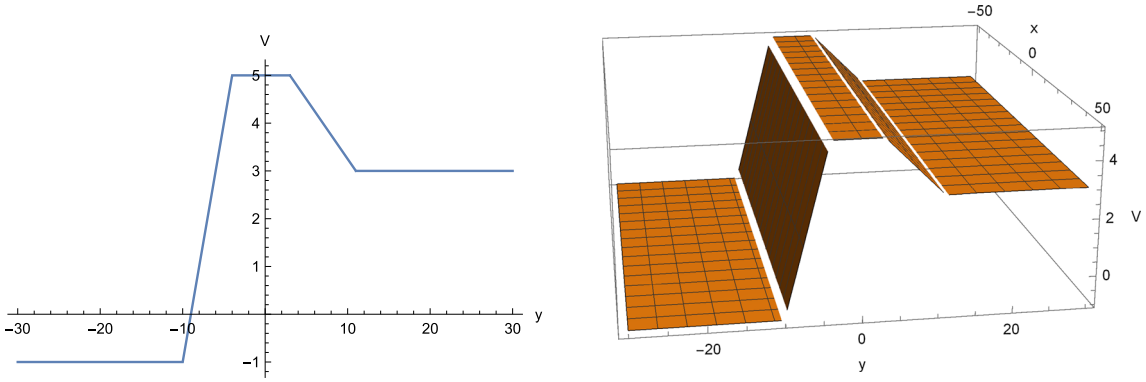

Fig. 2 Generic potential with parameters $\{y_{\rm L},\ y'_{\rm L},\ y'_{\rm R},\ y_{\rm R}\} = \{-10,\ -4,\ 3,\ 11\}$ and $\{V_{\rm L},\ V_0,\ V_{\rm R}\} = \{-1,\ 5,\ 3\}$ in arbitrary units. A 3D picture is shown, too

The density and flux of probabilities are given by the components of the 3-current

$$\begin{aligned} J^\mu(x) &= \bar\Psi(x)\gamma^\mu\Psi(x),\\ \rho(t,\mathbf{x}) &= J^0(t,\mathbf{x}) = \Psi^\dagger(t,\mathbf{x})\Psi(t,\mathbf{x}),\\ J^i(t,\mathbf{x}) &= \Psi^\dagger(t,\mathbf{x})\alpha^i\Psi(t,\mathbf{x}),\quad i=1,2. \end{aligned} \tag{3.3}$$

In order to compare the theory with the classical one we will need to compute the mean position and velocity of the particle, which we will denote by $\mathbf{x}_{\rm q} = (x_{\rm q}, y_{\rm q})$ and $\mathbf{v}_{\rm q} = (v_{\rm q}^x, v_{\rm q}^y)$, respectively. In a general state described by a (normalizable) vector $|\Psi\rangle\,(t)$, the mean velocity is given by

$$v^i_{\rm q}(t) = \frac{1}{||\Psi||^2}\left\langle\Psi|\alpha^i|\Psi\right\rangle(t),\quad i=1,2, \tag{3.4}$$

and the mean position by integrating each side of the latter equation. This expression amounts to integrate the fluxes J^i and divide by the integral of the density ρ given in (3.3).

However, when dealing with (non-normalizable) stationary scattering states, we will use the following alternative. We first define "local mean velocities"

$$v^i_{\rm q}(\mathbf{x}) = J^i(\mathbf{x})/\rho(\mathbf{x}), \tag{3.5}$$

and then find the mean position $x^i_{\rm q}(t)$ by integrating with suitable boundary conditions the differential equations

$$\dot x^i_{\rm q}(t) = v^i_{\rm q}(\mathbf{x}_{\rm q}(t)), \tag{3.6}$$

where a dot means time differentiation.

In this section, we restrict ourselves to the special case of a potential depending only on the y-coordinate: $V = V(y)$, the electric field $\mathbf{E}(y) = (0,\ -V'(y))$ being parallel to the y-axis. Moreover, the electric field is assumed to vanish outside of an interval $y_{\rm L} \le y \le y_{\rm R}$. More precisely, the potential obeys the conditions

$$V(y) = \begin{cases} V_{\rm L}, & y \le y_{\rm L},\\ V_{\rm R}, & y \ge y_{\rm R}, \end{cases} \tag{3.7}$$

where $V_{\rm L}$ and $V_{\rm R}$ are constant. An illustration is provided by Fig. 2 below.

We take the two-component Dirac spinor to be stationary and, due to the x-independence of the potential, to be an eigenvector of the x-momentum component, with eigenvalue k_x:

$$\Psi(t,x,y) = \begin{pmatrix}\Phi_1(t,x,y)\\ \Phi_2(t,x,y)\end{pmatrix} = e^{-i\omega t + ik_x x}\begin{pmatrix}f(y)\\ g(y)\end{pmatrix}, \tag{3.8}$$

where ω is an eigenvalue of the Dirac Hamiltonian operator (3.2). The functions $f(y)$ and $g(y)$ then obey the equations

$$\begin{aligned} i(V(y)-\omega)f(y) - k_x g(y) + g'(y) = 0,\\ i(V(y)-\omega)g(y) + k_x f(y) + f'(y) = 0, \end{aligned} \tag{3.9}$$

and the probability density and flux read

$$\begin{aligned} \rho(y) &= f^*(y)f(y) + g^*(y)g(y)\\ J^x(y) &= i\left(f^*(y)g(y) - g^*(y)f(y)\right),\\ J^y(y) &= f^*(y)g(y) + g^*(y)f(y), \end{aligned} \tag{3.10}$$

where * means complex conjugation. In the present case, the local velocity (3.5) entering in the differential equation (3.6) depends only on the coordinate $y_q(t)$.

3.1.1 Asymptotic states

Outside of the interval $y_{\rm L} < y < y_{\rm R}$, the wave function obeys the Dirac equations (3.9) with a constant electrostatic potential, denoted by V in the present subsection. Its solutions are progressive waves $(f^V_\pm,\ g^V_\pm)$, where the suffix $\pm$ means right or left mode, respectively. Up to an overall factor:

$$f_{\pm}^{V}(y) = e^{\pm ik_y y}, \quad g_{\pm}^{V}(y) = \frac{\pm k_y - ik_x}{\omega - V} e^{\pm ik_y y}, \tag{3.11}$$

with $k_y = \sqrt{(\omega - V)^2 - k_x^2}$, if $(\omega - V)^2 > k_x^2$ (see Fig. 1(a)). If $(\omega - V)^2 < k_x^2$, the waves are real exponentials, hence do not propagate:

$$f_{\pm}^{V}(y) = e^{\pm \kappa y}, \quad g_{\pm}^{V}(y) = -i \frac{k_x \pm \kappa}{\omega - V} e^{\pm \kappa y}, \tag{3.12}$$

with $\kappa = \sqrt{k_x^2 - (\omega - V)^2}$.

In the propagating case (3.11) the (unnormalized) probability density and fluxes (3.10) are explicitly given by

$$\rho_{\pm} = 2, \quad J_{\pm}^{x} = \frac{2k_x}{\omega - V}, \quad J_{\pm}^{y} = \pm \frac{2k_y}{\omega - V}, \tag{3.13}$$

which leads to the mean velocities (see (3.5))

$$v_{\pm}^{x} = \frac{k_x}{\omega - V}, \quad v_{\pm}^{y} = \pm \frac{k_y}{\omega - V}, \quad \text{with } (v_{\pm}^{x})^2 + (v_{\pm}^{y})^2 = 1. \tag{3.14}$$

Note that, thinking in the context of condensed matter, for $\omega < V$, i.e., for a negative kinetic energy, the propagation may be considered as of a particle in the (non-full) valence band (VB), whereas it is of a particle of positive kinetic energy in the (non-empty) conduction band (CB) if $\omega > V$. In the former case, the direction of the flux, equal to that of the mean velocity, is opposed to that of the phase velocity, the latter being proportional to $\mathbf{k}$. This means that a right (left) mode as defined above corresponds in fact to a left (right) moving particle.

Similar considerations can be made in the case of the propagation of holes.

3.1.2 Scattering boundary conditions

The free particle solutions (3.11) and (3.12), with k_y and κ substituted by

$$k_{y\mathrm{L,R}} = \sqrt{(\omega - V_{\mathrm{L,R}})^2 - k_x^2}, \quad \kappa_{\mathrm{L,R}} = \sqrt{k_x^2 - (\omega - V_{\mathrm{L,R}})^2}, \tag{3.15}$$

will be used in the following for the prescription of the asymptotic behaviour of the solutions of the Dirac equations (3.9) in the cases of potentials obeying the condition (3.7). Interested in scattering states, we choose boundary conditions such that we have a pure right moving particle state in the right asymptotic region $y \geq y_{\mathrm{R}}$. In the case of a CB state, these conditions will be taken as

$$f(\bar{y}) = f_{+}^{V_{\mathrm{R}}}(\bar{y}), \quad g(\bar{y}) = g_{+}^{V_{\mathrm{R}}}(\bar{y}), \tag{3.16}$$

for the wave functions f, g solutions of the interacting Dirac equation, where $\bar{y} \geq y_{\mathrm{R}}$ is some normalization point chosen in the right asymptotic region, $f_{+}^{V_{\mathrm{R}}}$ and $g_{+}^{V_{\mathrm{R}}}$ are the asymptotic wave functions defined in (3.11), with $k_y = k_{y\mathrm{R}}$. For a VB state, one has to substitute the index $+$ by the index $-$. These conditions correspond to a process consisting of an incoming particle coming from the left region $y \leq y_{\mathrm{L}}$: hence, in the right region $y \geq y_{\mathrm{R}}$, one admits only the solution with flux pointing to the right – hence a positive wave vector component k_y for an outgoing CB particle and a negative one for a VB particle. In the left region both directions (incoming and reflecting) are allowed. Again we have to distinguish the motions of a CB or of a VB particle. The proper distinction between CB and VB particles is crucial for the correct solution of the Klein phenomenon [2–5,42,43,55], as mentioned in the Introduction.

The above holds for $k_{y\mathrm{R}}$ real. If, on the other hand, $k_{y\mathrm{R}}$ is imaginary, one has no propagating state in the right region. Therefore the boundary condition must select from (3.12) the exponentially decreasing solution to be put in the boundary condition:

$$f(\bar{y}) = f_{-}^{V_{\mathrm{R}}}(\bar{y}), \quad g(\bar{y}) = g_{-}^{V_{\mathrm{R}}}(\bar{y}), \tag{3.17}$$

with $\kappa = \kappa_{\mathrm{R}}$ (see (3.15)).

The conditions (3.16) or (3.17) define uniquely the solution of the Dirac equation with interaction.

3.1.3 Reflection and transmission coefficients

The reflection and transmission probabilities $\mathcal{R}$ and $\mathcal{T}$ are given, in the present case of an x-independent potential, by the expressions

$$\mathcal{R} = \frac{|J_{\mathrm{L}-}^{y}|}{|J_{\mathrm{L}+}^{y}|}, \quad \mathcal{T} = \frac{|J_{\mathrm{R}+}^{y}|}{|J_{\mathrm{L}+}^{y}|}, \tag{3.18}$$

where $J_{\mathrm{L}+}^{y}$, $J_{\mathrm{L}-}^{y}$ and $J_{\mathrm{R}+}^{y}$ are the y-components of the incoming, reflecting and outgoing probability fluxes, respectively, in the asymptotic region. Note that $J_{\mathrm{R}-}^{y} = 0$ in our scattering setting. Remember that, if $\omega - V_{\mathrm{L}} < 0$, respectively $\omega - V_{\mathrm{R}} < 0$, we have a VB particle propagating and the flux is in the direction opposed to that of the wave vector, in the left, respectively right, region. Due to the t and x independence of the potential, the continuity equation for the density and flux reads $dJ_y(y)/dy = 0$, hence $J_{\mathrm{L}+}^{y} + J_{\mathrm{L}-}^{y} = J_{\mathrm{R}+}^{y}$, which ensures the probability conservation $\mathcal{R} + \mathcal{T} = 1$. Note that in the gap $V_{\mathrm{R}} - |k_x| < \omega < V_{\mathrm{R}} + |k_x|$ there is full opacity: $R = 1, T = 0$.

The fluxes are calculated according to (3.10) in terms of the incoming, reflecting and outgoing wave functions obtained from the Fourier coefficients of the wave function

component[7] $f(y)$ in the corresponding asymptotic regions (where the waves are free ones, the potential being constant):

$$a_{\mathrm{L}\pm} = \frac{k_{y\mathrm{L}}}{2\pi}\int_{y_\mathrm{L}-2\pi/k_{y\mathrm{L}}}^{y_\mathrm{L}} dy\, e^{\mp i k_{y\mathrm{L}} y} f(y),$$
$$a_{\mathrm{R}\pm} = \frac{k_{y\mathrm{R}}}{2\pi}\int_{y_\mathrm{R}}^{y_\mathrm{R}+2\pi/k_{y\mathrm{R}}} dy\, e^{\mp i k_{y\mathrm{R}} y} f(y). \tag{3.19}$$

Let us calculate, as an example, the flux $J^y_{\mathrm{L}+}$ for the incoming mode (in the region $y \le y_\mathrm{L}$), in the case of a CB particle, i.e., with $\omega > V_\mathrm{L}$). The relevant spinor components are given by (3.11), with "±" substituted by "+" and multiplied by the Fourier coefficient $a_{\mathrm{L}+}$. This flux then is given by the last of Eq. (3.13), but multiplied by $|a_+|^2$. Doing the same for the other fluxes, we obtain the result (for incoming and outgoing **CB particle** states

$$J^y_{\mathrm{L}\pm} = \pm|a_{\mathrm{L}\pm}|^2\frac{2k_{y\mathrm{L}}}{\omega - V_\mathrm{L}}, \quad J^y_{\mathrm{R}\pm} = \pm|a_{\mathrm{R}\pm}|^2\frac{2k_{y\mathrm{R}}}{\omega - V_\mathrm{R}}, \tag{3.20}$$

observing that $a_{\mathrm{R}-} = J^y_{\mathrm{R}-} = 0$ due to the scattering boundary conditions (3.16). For incoming or/and outgoing **VB particle** states one has to substitute $a_{\mathrm{L,R}\pm}$ by $a_{\mathrm{L,R}\mp}$ in the right-hand side of the first or/and second of Eq. (3.20). This result allows then to compute the reflection and transmission coefficients (3.18).

Observe that these calculations concern scattering states characterized with both $k_{y\mathrm{L}}$ and $k_{y\mathrm{R}}$ (see (3.15)) being real numbers. We discard the case of $k_{y\mathrm{L}}$ being imaginary, since this would mean the absence of an incoming mode. On the other hand, if $k_{y\mathrm{R}}$ turns out to be imaginary, the boundary condition (3.16) selects the solution which is exponentially decreasing in the region $y \ge y_\mathrm{R}$. In this case, obviously, $\mathcal{T} = 0$ and $\mathcal{R} = 1$.

Bound states characterized by $k_{y\mathrm{L}}$ and $k_{y\mathrm{R}}$ both being imaginary – such the bound states of a particle inside a potential well – will not be considered in this paper.

3.1.4 Comparison with the classical motion

The relevant quantities which can thus be calculated are, beyond the wave functions, the fluxes (3.10), the reflection and transmission coefficients $\mathcal{R}$ and $\mathcal{T}$, and the mean velocities (3.5) or, after integration, the mean trajectories. As a check of the "correspondence principle", we can compare the quantum mean velocities and trajectories with the ones obtained from the classical theory.

[7] We could as well choose the other component, $g(y)$, without changing the result.

Classical velocities and trajectories are solutions of the equations of motion (B.1) and (B.2) of Appendix B with the appropriate boundary conditions

$$x_{\mathrm{cl}}(\bar t) = x_\mathrm{q}(\bar t) = \bar x, \quad y_{\mathrm{cl}}(\bar t) = y_\mathrm{q}(\bar t) = \bar y,$$
$$\dot x_{\mathrm{cl}}(\bar t) = \dot{\bar x} = v^x_\mathrm{q}(\bar t), \tag{3.21}$$

taken at some time $\bar t$. $(\bar x,\ \bar y)$ is some suitable normalization point, with $\bar y \le y_\mathrm{L}$ if a reflection mode is considered, or $\bar y \ge y_\mathrm{R}$ in the case of a transmission mode. $\dot{\bar x} = v^x_\mathrm{q}(\bar t)$ is the x component of the mean quantum velocity at time $\bar t$. The indices "cl" and "q" refer to classical quantities and quantum mean values, respectively.

3.2 Some examples

Results for some particular potentials are presented in this Section. These potentials are of the square type or, more generally, piece-wise continuous functions $V(y)$ of the form (see Fig. 2)

$$V(y) = \begin{cases} V_\mathrm{L}, & y \le y_\mathrm{L}, \\ \dfrac{V_0 - V_\mathrm{L}}{y'_\mathrm{L} - y_\mathrm{L}}(y - y_\mathrm{L}) + V_\mathrm{L}, & y_\mathrm{L} \le y \le y'_\mathrm{L} \\ V_0, & y'_\mathrm{L} \le y \le y'_\mathrm{R} \\ \dfrac{V_\mathrm{R} - V_0}{y_\mathrm{R} - y'_\mathrm{R}}(y - y_\mathrm{R}) + V_\mathrm{R}, & y'_\mathrm{R} \le y \le y_\mathrm{R} \\ V_\mathrm{R}, & y_\mathrm{R} \le y \end{cases} \tag{3.22}$$

The electric field is oriented in the y-direction, with its value given by $E = -\dfrac{V_0 - V_\mathrm{L}}{y'_\mathrm{L} - y_\mathrm{L}}$ in the interval $(y_\mathrm{L}, y'_\mathrm{L})$, by $E = -\dfrac{V_0 - V_\mathrm{R}}{y'_\mathrm{R} - y_\mathrm{R}}$ in the interval $(y'_\mathrm{R}, y_\mathrm{R})$ and by $E = 0$ outside.

The potential (3.22) will be substituted by a smoothed one in the numerical applications, in order to avoid problems caused by the singularities at y_L, y'_L, y'_R and y_R.

In each of the examples shown below, the Dirac equation is solved using the scattering boundary conditions (3.16) or (3.17) explained in Sect. 3.1.2: the incoming wave describes a particle emitted from the left half plane $y \le y_\mathrm{L}$ (the left region with flat potential), producing a reflected wave to the left and a transmitted wave to the right describing the transmitted particle – or, depending on the energy and momentum parameters, an exponentially decreasing wave corresponding to full opacity of the potential step or barrier.

3.2.1 Square step potential

This is a slight generalization to 2 dimensions of the one-dimensional potential step problem found in the standard

literature [2,43,55], with the y-dependent potential

$$V(y) = \begin{cases} 0, & y < 0, \\ V > 0, & y > 0, \end{cases} \tag{3.23}$$

The solution of the Dirac equation as an eigenvector of the energy with value ω, and of the x-component of the linear momentum with value k_x (see (3.8)), and with the scattering boundary condition defined in Sect. 3.1.2, is given, in the case of a **particle** in both sides, i.e., with $\omega > V$, by[8]

$$\Psi(t,x,y) = \begin{cases} e^{-i\omega t + ik_x x} \begin{pmatrix} f_+^{\mathrm{L}}(y) + A f_-^{\mathrm{L}}(y) \\ g_+^{\mathrm{L}}(y) + A g_-^{\mathrm{L}}(y) \end{pmatrix} & (y < 0), \\ e^{-i\omega t + ik_x x} \begin{pmatrix} B f_-^{\mathrm{R}}(y) \\ B g_-^{\mathrm{R}}(y) \end{pmatrix} & (y > 0), \end{cases} \tag{3.24}$$

where A and B are coefficients fixed by the continuity condition

$$\Psi(t,x,y)|_{y=-0} = \Psi(t,x,y)|_{y=+0},$$

with the result[9]

$$A = \begin{cases} \dfrac{k_{y\mathrm{L}}(\omega - V - m) - k_{y\mathrm{R}}(\omega - m) - ik_x V}{k_{y\mathrm{L}}(\omega - V - m) + k_{y\mathrm{R}}(\omega - m) + ik_x V}, & \omega < 0, \\ \dfrac{-k_{y\mathrm{L}}(\omega - V - m) + k_{y\mathrm{R}}(\omega - m) - ik_x V}{k_{y\mathrm{L}}(\omega - V - m) + k_{y\mathrm{R}}(\omega - m) + ik_x V}, & 0 < \omega < V, \\ \dfrac{k_{y\mathrm{L}}(\omega - V - m) - k_{y\mathrm{R}}(\omega - m) + ik_x V}{k_{y\mathrm{L}}(\omega - V - m) + k_{y\mathrm{R}}(\omega - m) - ik_x V}, & \omega > V, \end{cases} \tag{3.25}$$

$$B = \begin{cases} \dfrac{2k_{y\mathrm{L}}(\omega - m)}{k_{y\mathrm{L}}(\omega - V - m) + k_{y\mathrm{R}}(\omega - m) + ik_x V}, & \omega < 0, \\ \dfrac{2k_{y\mathrm{L}}(\omega - m)}{k_{y\mathrm{L}}(\omega - V - m) - k_{y\mathrm{R}}(\omega - m) - ik_x V}, & 0 < \omega < V, \\ \dfrac{2k_{y\mathrm{L}}(\omega - m)}{k_{y\mathrm{L}}(\omega - V - m) + k_{y\mathrm{R}}(\omega - m) - ik_x V}, & \omega > V, \end{cases} \tag{3.26}$$

where the y-components $k_{y\mathrm{L}}$ and $k_{y\mathrm{R}}$ of the wave vector are given by (3.15) with $V_{\mathrm{L}} = 0$ and $V_{\mathrm{R}} = V$.

The reflection and transmission coefficient (3.18) take then the form

$$\mathcal{R} = |A|^2 = \begin{cases} \dfrac{\left(-k_{y\mathrm{L}}(\omega - V - m) + k_{y\mathrm{R}}(\omega - m)\right)^2 + k_x^2 V^2}{\left(k_{y\mathrm{L}}(\omega - V - m) + k_{y\mathrm{R}}(\omega - m)\right)^2 + k_x^2 V^2}, & \omega < -\sqrt{k_x^2 + m^2}, \\ \dfrac{\left(k_{y\mathrm{L}}(\omega - V - m) + k_{y\mathrm{R}}(\omega - m)\right)^2 + k_x^2 V^2}{\left(-k_{y\mathrm{L}}(\omega - V - m) + k_{y\mathrm{R}}(\omega - m)\right)^2 + k_x^2 V^2}, & \sqrt{k_x^2 + m^2} < \omega < V - \sqrt{k_x^2 + m^2}, \\ 1, & V - \sqrt{k_x^2 + m^2} < \omega < V + \sqrt{k_x^2 + m^2}, \\ \dfrac{\left(-k_{y\mathrm{L}}(\omega - V - m) + k_{y\mathrm{R}}(\omega - m)\right)^2 + k_x^2 V^2}{\left(k_{y\mathrm{L}}(\omega - V - m) + k_{y\mathrm{R}}(\omega - m)\right)^2 + k_x^2 V^2}, & \omega > V + \sqrt{k_x^2 + m^2}, \end{cases} \tag{3.27}$$

and

$$\mathcal{T} = |B|^2 \frac{k_{y\mathrm{R}}(\omega - V - m)}{k_{y\mathrm{L}}(\omega - m)} = 1 - \mathcal{R} \tag{3.28}$$

We note that in the cases where $-\sqrt{k_x^2 + m^2} < \omega < \sqrt{k_x^2 + m^2}$ or $V - \sqrt{k_x^2 + m^2} < \omega < V + \sqrt{k_x^2 + m^2}$, the wave vector components $k_{y\mathrm{L}}$ or $k_{y\mathrm{R}}$, respectively, are imaginary, which corresponds to real exponential waves. The first case is discarded since there is then no propagating incident particle. In the second case, there is no transmitted propagating particle, hence the reflection probability $\mathcal{R}$ is equal to 1.

One checks that $\mathcal{R} + \mathcal{T} = 1$, as it should.

One recovers the standard literature result [2] for the 1-dimensional system by taking $k_x = 0$ in (3.27), (3.28), i.e., a vanishing x-component of the wave vector.

Let us note, at this point, that the result, taken at $k_x = 0$, does not coincide with the expression produced in part of the literature [2–5]. The latter gives values for $\mathcal{R}$ and $\mathcal{T}$ outside of the interval (0, 1), a fact called the "Klein paradox". As it is explained in [2] this apparent paradox appears if one forgets that VB particle propagation occurs in the Dirac theory at values of the energy for which the non-relativistic quantum theory would yield an exponential damping. This is what happens, in the present example, for the incident, reflected or transmitted object if $\omega < -\sqrt{k_x^2 + m^2}$, and for the transmitted one if $\sqrt{k_x^2 + m^2} < \omega < V - \sqrt{k_x^2 + m^2}$. On the other hand, there is exponential damping if $V - \sqrt{k_x^2 + m^2} < \omega < V + \sqrt{k_x^2 + m^2}$.

Figure 3 shows the behaviour of the reflection probability as a function of the energy ω for three sets of parameters' values. One observes an increase of the forbidden region and of the region of total reflection when either $|k_x|$ or m increases.

3.2.2 Square barrier potential

This is again a slight generalization to 2 dimensions of the problem of the one-dimensional potential barrier [2], with the y-dependent potential

$$V(y) = \begin{cases} 0, & y < -a \text{ or } y > a \ (a > 0), \\ V > 0, & -a < y < a, \end{cases} \tag{3.29}$$

[8] Recall that the suffixes + and − refer to the sign of the phase velocity as defined in Eq. (3.11).

[9] In this and the next subsection, we consider a massive particle for the sake of comparison with the literature [2–5].

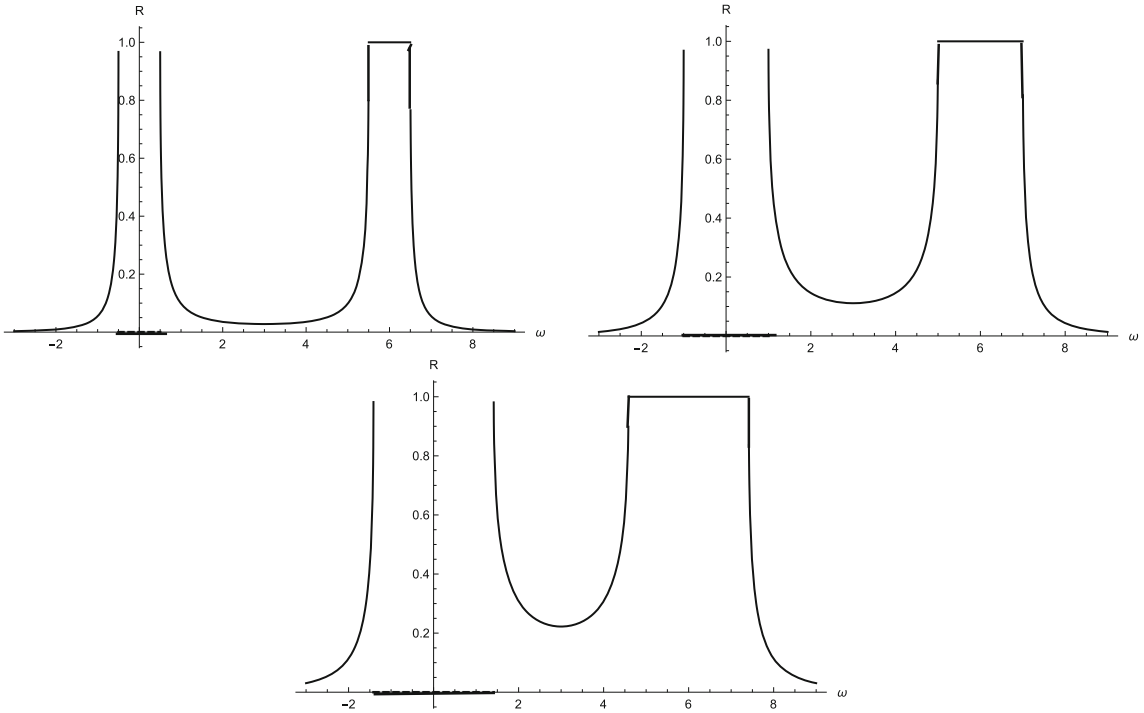

Fig. 3 Square step potential (3.23) with $V = 6$: reflection probability $\mathcal{R}$ as a function of the frequency ω for $(m, k_x) = (0, 0.5)$, $(0, 1.0)$ and $(1.0, 1.0)$, respectively. The heavy horizontal segment shows the energy gap interval

The solution of the (massive) Dirac equation as well as the calculation of the reflection and transmission probabilities $\mathcal{R}$ and $\mathcal{T}$ follow the same lines as for the potential step in the preceding subsection and will not be detailed here. The results for $\mathcal{R}$ and $\mathcal{T}$ happen to coincide with the solution found in [2] for the 1-dimensional problem,[10] but with the mass parameter m substituted by $\sqrt{k_x^2 + m^2}$:

$$\mathcal{R} = \frac{(1-\lambda)^2 \sin^2(2ak_y)}{4\lambda + (1-\lambda)^2 \sin^2(2ak_y)}, \qquad \mathcal{T} = 1 - \mathcal{R}, \tag{3.30}$$

with $k_y = \sqrt{(\omega - V)^2 - k_x^2 - m^2}$ and

$$\lambda = \frac{(V - \omega + \sqrt{k_x^2 + m^2})(\omega + \sqrt{k_x^2 + m^2})}{(V - \omega - \sqrt{k_x^2 + m^2})(\omega - \sqrt{k_x^2 + m^2})},$$

for $\omega > \sqrt{k_x^2 + m^2}$ (propagation of a CB particle) or $\omega < -\sqrt{k_x^2 + m^2}$ (propagation of an VB particle). These probabilities are not defined in the gap interval $-\sqrt{k_x^2 + m^2} < \omega < \sqrt{k_x^2 + m^2}$, where there is no propagation at all.

Figure 4 shows the behaviour of the reflection probability $\mathcal{R}$ as a function of the energy ω for three sets of parameters' values in the massless case. One observes a decrease of the forbidden region when $|k_x|$ decreases. As can be seen from (3.30), for a vanishing momentum x-component, i.e., for a frontal incidence, there is total transparency: $\mathcal{R} = 0$ for $k_x = 0$. The oscillations in the allowed region correspond to the so-called transmission resonance phenomenon [2].

[10] This is not the case in the example of the step potential examined in the preceding subsection, where $\mathcal{R}$ and $\mathcal{T}$ depend on both independent variables k_x and m.

3.2.3 *Oblique step potential*

We consider here the stepwise potential $V(y)$, a smoothed version of the one shown in Fig. 5. In this example and in the next ones, the massless Dirac equation (3.1) as well as the dynamical quantities of interest are solved and calculated numerically using the software Mathematics [47].

Figure 6 shows the reflection probability $\mathcal{R}$ as a function of the energy ω for various values of the x-component k_x of the momentum.

One observes features very similar to those of the square step potential seen in Sect. 3.2.1. Besides the expected energy gap, one recovers the "Klein phenomenon": Complete opacity for energies in the region $V_R - |k_x| < \omega < V_R + |k_x|$, and appreciable transparency in the region $V_L + |k_x| < \omega < V_R - |k_x|$ where opacity would be complete in the non-relativistic theory. Recall that V_L and V_R are the values of the potential in the left and right region, respectively. Also, as in the square step case, the transparency tends to increase when the absolute value of $|k_x|$ decreases, being complete for $k_x = 0$, i.e., for an incident wave vector orthogonal to the potential barrier.

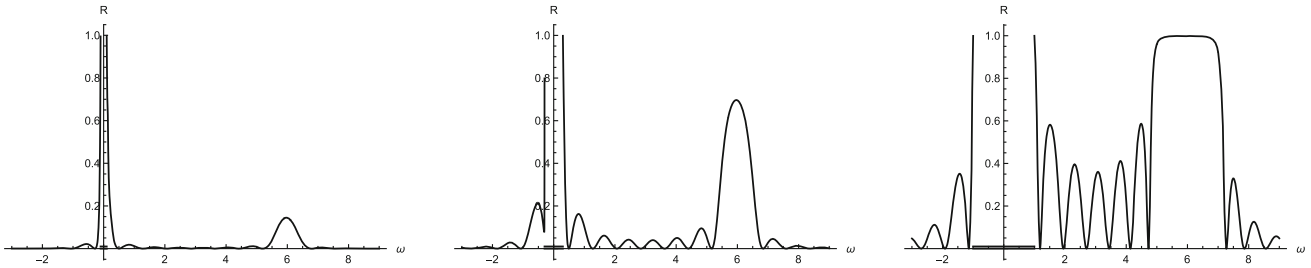

Fig. 4 Square barrier potential (3.29): reflection probability $\mathcal{R}$ as a function of the frequency ω in the massless case for $k_x = 0.1$, 0.3 and 1.0, respectively. The heavy horizontal segment shows the energy gap interval. The potential parameters are $V = 6$ and $a = 5$

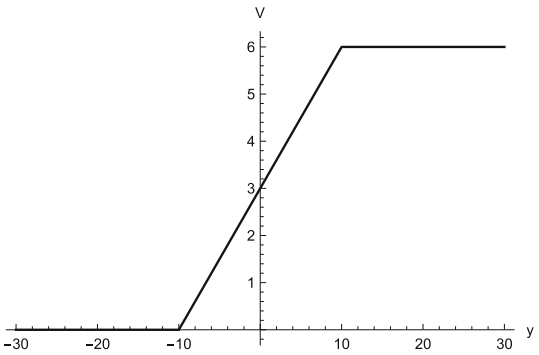

Fig. 5 Oblique step potential. The values of the parameters of (3.22) are taken as $y'_L = y'_R = y_R = 10$, $V_{\rm L} = 0$, $V_0 = V_{\rm R} = 6$

Figure 7 shows the quantum mean trajectories compared with the corresponding classical ones for one value of k_x and three values of the energy ω. We show in the left part of the graphics both the incident and reflected particle quantum paths, with arrows indicating the direction of the mean velocity vector. In the right-hand part only the transmitted particle path appears, by construction, due to the boundary conditions corresponding to an incident particle coming from the left.

The first case shown in Fig. 7 exemplifies the case of the energy lying between the bottom and top values $(V_{\rm L}, V_{\rm R}) = (0, 6)$ of the potential, where the reflection is appreciable – it would be total in the classical case. The incoming and reflection modes are those of a CB particle, whereas the transmitted one is that of a VB particle. On the classical level, there are corresponding trajectories both for the reflection of a CB particle coming from the left or for a VB particle coming from the right. Both are shown in the figure as dashed lines. We see that the quantum mean trajectories follow the classical paths whenever there are given by pure left or right progressive waves, as it is the case outside of the interaction domain $(y_{\rm L}, y_{\rm R}) = (-10, 10)$. Inside this domain, one sees a somewhat wild behaviour of the quantum trajectory – a *Zitterbewegung* effect due to the superposition of right moving and left moving waves. However, when y approaches $y_{\rm R}$ from below, the trajectory becomes increasingly smooth and coincident with the classical one or, in other words, becomes a more and more pure right moving mode.

The other two cases shown in Fig. 7, with small reflection probabilities, are typical scattering states, the energy being above the top value of the potential, $\omega > V_{\rm R}$. There is no reflected classical trajectory, but only one corresponding to the transmitted particle. The *Zitterbewgung* of the quantum mean trajectory is still visible in the intermediary region $(y_{\rm L}, y_{\rm R})$, but it clearly diminishes for higher and higher energies above the top potential value $V_{\rm R}$, together with an improvement of the coincidence of the quantum trajectory with the classical one.

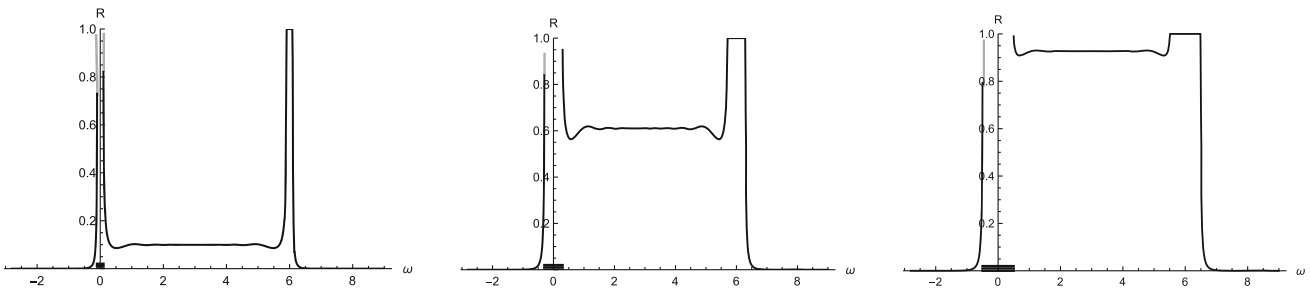

Fig. 6 Potential of Fig. 5: reflection probability $\mathcal{R}$ as a function of the frequency ω in the massless case for $k_x = 0.1$, 0.3 and 0.5, respectively. The heavy horizontal segment shows the energy gap interval

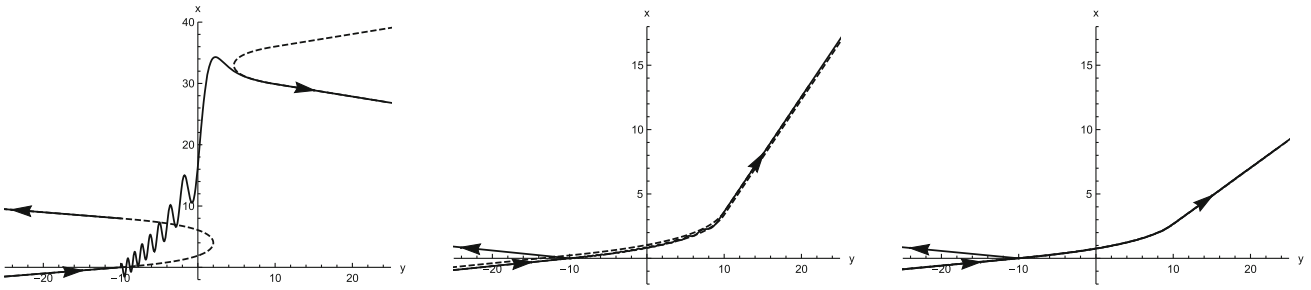

Fig. 7 Potential of of Fig. 5: quantum mean trajectories (continuous lines) are shown together with the corresponding classical trajectories (dashed lines), for $(\omega, k_x) = (4.0, 0.4)$, $(6.6, 0.4)$ and $(7.0, 0.4)$. The respective values of the reflection probability $\mathcal{R}$ are 0.812, 0.021 and 0.008

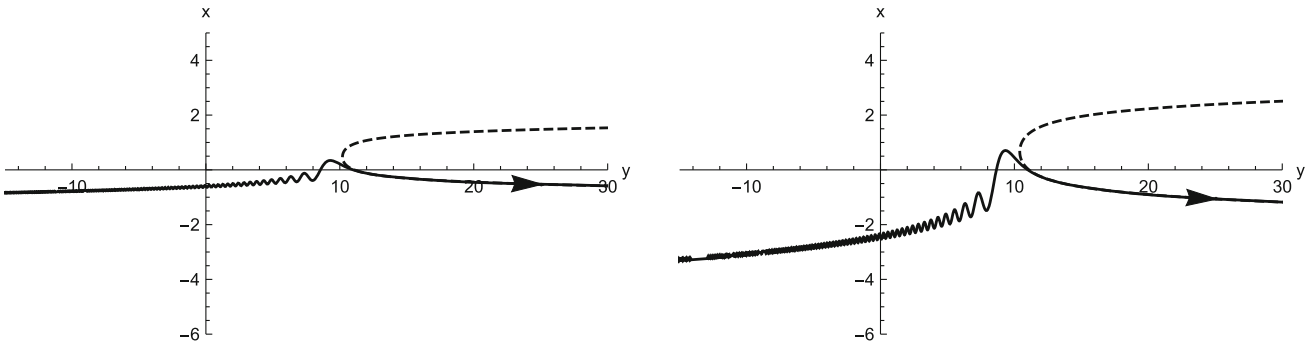

Fig. 8 Step potential as specified in the text, with a large scale parameter $L = 900$. Quantum mean trajectory for a CB particle coming from the left and emerging after the potential barrier as a VB particle is shown. The dashed line shows the classical trajectory of a particle of negative kinetic energy coming from the right and repelled by the same electric field. $(\omega, k) = (10.0,\ 0.2)$ and $(10.0,\ 0.4)$

3.2.4 Approximatively constant electric field

The interaction of the particle of charge q with a constant electric field E in the y direction would be given by the potential

$$V(\mathbf{x}) = -qEy. \tag{3.31}$$

Nevertheless, in order to take advantage of the calculation apparatus used in the preceding subsection, we simulate the situation with an oblique step potential whose domain of non-triviality extends to large positive and negative values of the y coordinate. More specifically, we choose the following expressions for the potential parameters defined in Fig. 2: $\{y_{\mathrm{L}},\ y'_{\mathrm{L}},\ y'_{\mathrm{R}},\ y_{\mathrm{R}}\} = \{-L,\ L,\ L,\ L\}$ and $\{V_{\mathrm{L}},\ V_0,\ V_{\mathrm{R}}\} = \{-L,\ L,\ L\}$, where the scale L is "large". This means that, the charge of the particle being $q = 1$, we have a constant electric field $E = -1$ in the interval $-L < y < L$, and $E = 0$ outside of this interval. Thus in a region which is reasonably small with respect to the scale L and located far from the boarder $\{-L, L\}$, as in Fig. 8, where L has been given the value 900, the behaviour of the particle must approximate the behaviour it would have for a really constant field. Moreover, in order to take into account the part of the trajectory where the quantum behaviour differs significantly from the classical one, we must take values for $|\omega/E|$ small with respect to the scale L. The coincidence of the quantum mean trajectory with the classical one is very good in the $y > |\omega/E|$ region, whereas no such comparison is possible in the left region because of the superposition of incoming and reflecting modes – which is the cause of the observed *Zitterbewegung*. The reflection probability $\mathcal{R}$ is shown in Table 1 for various values of k_x and one of ω. We have checked that the results are in fact practically independent of the energy ω if the order of magnitude of the latter is kept small with respect to the scale L. [It would be rigorously independent of ω in the case of a truly constant field as given by the potential (3.31)]. We also note that $\mathcal{R}$ grows with k_x. All of this is in qualitative accord with the *plateaux* in ω observed in the three examples shown in Fig. 6, as well as with the k_x dependence of these *plateaux*.

Table 1 Values of the reflection coefficient $\mathcal{R}$ for $\omega = 10$ and various values of k_x

k_x	0.0	0.1	0.2	0.4	0.8
$\mathcal{R}$	0.000	0.031	0.118	0.395	0.866

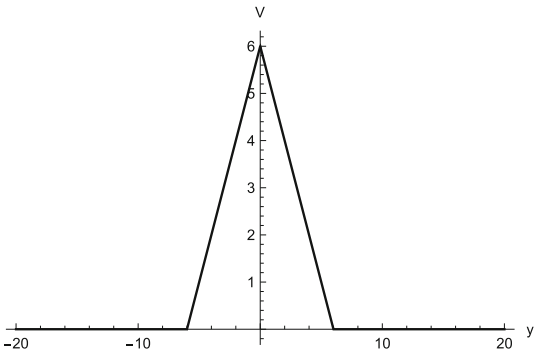

Fig. 9 Oblique barrier potential. The values of the parameters of (3.22) are taken as $y_{\rm L} = -6$, $y'_{\rm L} = y'_{\rm R} = 0$, $y_{\rm R} = 6$, $V_{\rm L} = V_{\rm R} = 0$, $V_0 = 6$

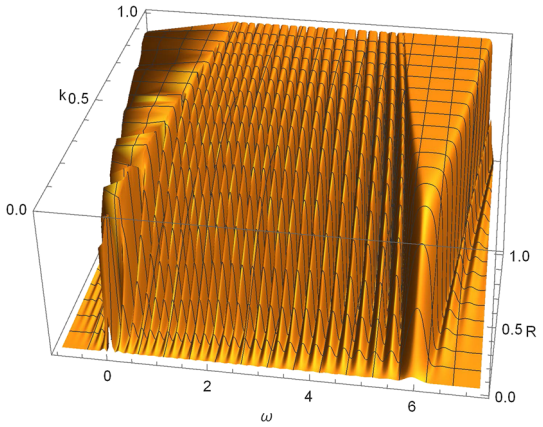

Fig. 12 Reflection probability $\mathcal{R}$ in function of ω and k_x for the potential barrier parameters $y_{\rm L} = -10$, $y'_{\rm L} = -4$, $y'_{\rm R} = 4$, $y_{\rm R} = 10$, $V_{\rm L} = V_{\rm R} = 0$, $V_0 = 6$ (see Eq. (3.22) and Fig. 2)

3.2.5 Oblique barrier potential

We consider now a barrier potential $V(y)$, a smoothed version of the one shown in Fig. 9. Figure 10 shows the reflection probability $\mathcal{R}$ as a function of the energy ω for various values of the x-component k_x of the momentum. The transmission resonance oscillations of the reflection coefficient $\mathcal{R}$ seen in the case of the square potential barrier (see Fig. 4) appear here, too. $\mathcal{R}$ oscillates between 0 (full transparency) to a maximum value which depends on the energy ω and tends to decrease together with the value of the momentum $x-$component k_x, going to 0 in the limit $k_x = 0$.

Figure 11 shows the quantum mean trajectories compared with the corresponding classical ones for one value of k_x and three values of the energy ω. For the first case, with a very small transmission probability, $\mathcal{T} = 0.087$, we show the classical trajectory of a incident particle from the left and reflected by a negative electric field, as well as that of an particle incoming from the right and reflected by a positive electric field. For the other two cases, where there is no reflection at the classical level, we show the trajectory of the classical particle going through.

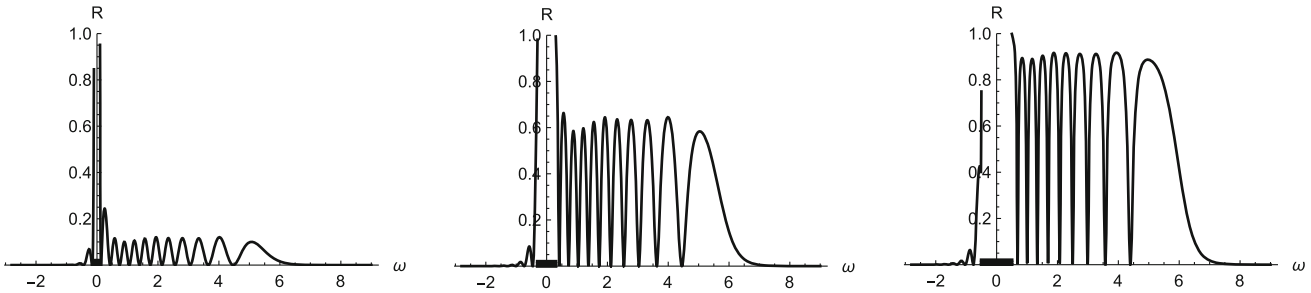

Fig. 10 Potential of Fig. 5: reflection probability $\mathcal{R}$ as a function of the frequency ω in the massless case for $k_x = 0.1$, 0.3 and 0.5, respectively. The heavy horizontal segment shows the energy gap interval

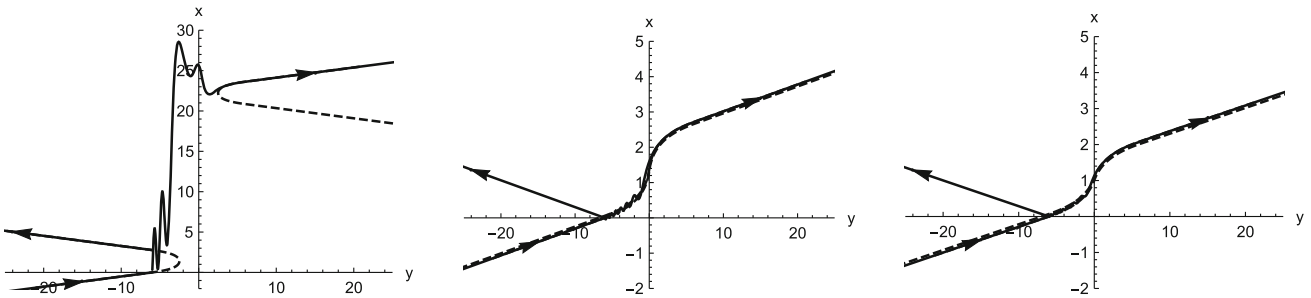

Fig. 11 Potential of Fig. 9: quantum mean trajectories (continuous lines) shown together with the corresponding classical trajectories (dashed lines), for $(\omega, k_x) = (4.0, 0.5)$, $(6.6, 0.5)$ and $(7.0, 0.5)$. The corresponding values of the reflection coefficient $\mathcal{R}$ are 0.913, 0.072 and 0.018, respectively

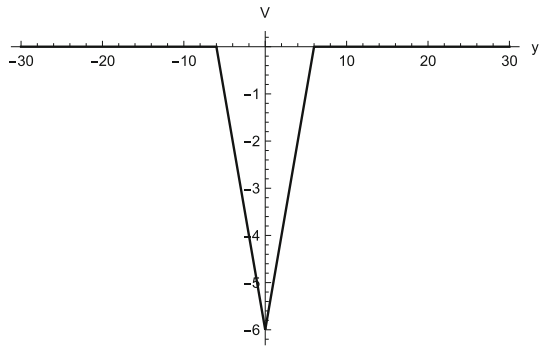

Fig. 13 Oblique well potential. The values of the parameters of (3.22) are taken as $y_L = -6$, $y'_L = y'_R = 0$, $y_R = 6$, $V_L = V_R = 0$, $V_0 = -6$

We observe a very good coincidence of the classical and mean quantum trajectories, with the exception, in the first case, of a small part of the interaction region where quantum effects are preponderant.

The classical trajectories in the first case exhibit the classical Klein phenomenon mentioned at the end of Appendix B: although the particle cannot go through the barrier, it may either come from the left and be repulsed to the left, having a positive kinetic energy, or it may either come from the right and be repulsed to the right having a negative kinetic energy.

Figure 12 shows the reflection probability $\mathcal{R}$ as a function of both the energy ω and the momentum component k_x, for another choice of the potential parameters.

3.2.6 Oblique well potential

The case of the well potential depicted in Fig. 13 is symmetric to that of the barrier potential of Sect. 3.2.5 due to the invariance of the theory under charge conjugation. This means, for the chosen parametrizations of both potentials, that a CB (or VB) particle of energy ω submitted to the barrier potential and VB (or CB) particle of energy $-\omega$ submitted to the well potential, both with the same value of the k_x component, will have a symmetric behaviour. In particular they will have equal reflection and transmission probabilities and follow symmetric mean quantum trajectories. The latter is exemplified by the comparison of the first graph of Fig. 11 with the first graph of Fig. 14. The second and third graphs of the latter figure show a particle flying over the well.

4 Conclusions

We have examined various examples of a relativistic quantum massless spinning particle in two-dimensional space, submitted to an electrostatic field oriented in one direction – the y-coordinate direction. These examples are characterized by y-dependent potentials of the form of a step, a barrier or a well. In each case we have computed the stationary solutions of the corresponding Dirac equation, together with the reflection and transmission coefficients. We have also computed in most cases the quantum mean trajectories and compared them with their classical counterparts, obtained by integration of the classical equations of motion, with boundary conditions adjusted to the quantum solution.

The explicit solutions found in the literature [2–5] concern a particle submitted to a square potential. Those of them which avoid the Klein "paradox" problem by properly taking into account the characteristics of the object being a CB or VB particle, i.e., a particle of positive or negative kinetic energy, turn out to coincide with ours. Examining the momentum and energy dependence of the reflection and transmission coefficients of our solutions for more general potentials such as smoothed oblique steps, barriers and wells, we found a behaviour of these coefficients which is qualitatively similar to that of the square potentials. In particular we reproduce explicitly in each case the Klein phenomenon of transmission at values of the energy for which the non-relativistic particle wave function would be exponentially damped through the barrier or behind the step.

Concerning the comparison of the quantum mean trajectories with the classical one, we found a very good agreement, excepted in situations where a non-negligible *Zitterbewe-*

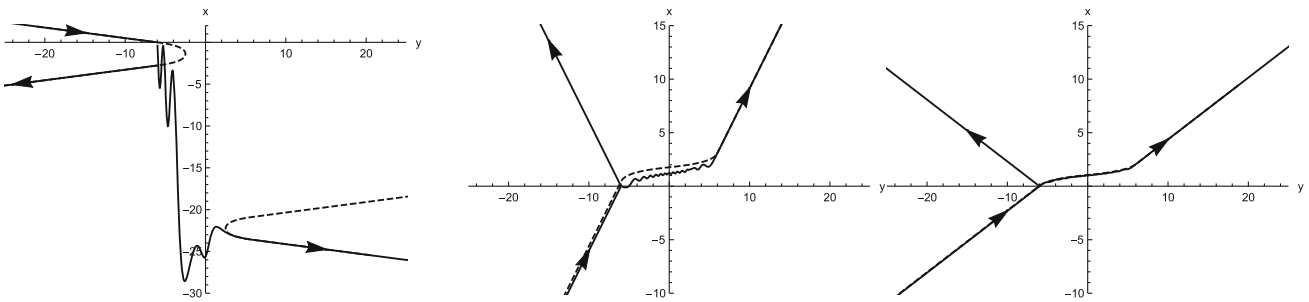

Fig. 14 Potential of Fig. 13: Quantum mean trajectories (continuous lines) shown together with the corresponding classical trajectories (dashed lines), for $(\omega, k_x) = (-4.0, 0.5)$, $(0.6, 0.5)$ and $(1.0, 0.5)$. The corresponding values of the reflection coefficient $\mathcal{R}$ are 0.913, 0.385 and 0.006, respectively

gung is present due to interference between right and left moving modes.

One important commentary on the Klein phenomenon which we observe in our calculations is still deserved, as, e.g., in the case of the potential of Fig. 5. In a non-relativistic theory, if the energy is below the top of the potential, there is no possibility of the particle to move in the right region, neither classically, nor quantically – excepted for an evanescent wave function in this region in the quantum case. As our calculations confirm, in the same setting, the transmission probability may be large in the relativistic case. It is of course zero in the classical relativistic theory, but there are solutions for the particle moving in the right region (see the first graphic of Fig. 7), with an acceleration opposed to the electric force due to a negative kinetic energy, which plays the role of an inertial factor. This is what we could call a "classical Klein phenomenon".

Acknowledgements This work was partially funded by the Conselho Nacional de Desenvolvimento Científico e Tecnológico—CNPq, Brazil (I.M., B. N., Z.O. and O.P.), by the Coordenação de Aperfeiçoamento de Pessoal de Nível Superior—CAPES, Brazil (I.M. and B.N.), by the Fundação de Amparo a Pesquisa do Estado de Minas Gerais - FAPEMIG, Brazil (O.P.) and by the Grupo de Sistemas Complejos de la Carrera de Física de la Universidad Mayor de San Andrés, UMSA, Bolivia (Z.O.), for their support.

Data Availability Statement This manuscript has associated data in a data repository. [Authors' comment: Computations in concrete cases are done with the help of the software Mathematica [47]. Interested readers may download (and use) the computer program from the arXiv site at the link https://arxiv.org/src/1910.03059v2/anc/Trajectories.nb and save it as a file: Trajectories.nb.]

Funded by SCOAP[3].

Appendices

A Notations and conventions

$$\begin{array}{ll}
\text{Units are such that} & c = \hbar = 1, \\
\text{Space-time coordinates:} & (x^\mu,\ \mu = 0, 1, 2), \\
& \mathbf{x} = (x^a,\ a = 1, 2), \\
\text{Space-time metric:} & \eta_{\mu\nu} = \text{diag}(1, -1, -1), \\
\text{Dirac matrices:} & \gamma^0 = \sigma_z,\ \gamma^x = i\sigma_x,\ \gamma^2 = i\sigma_y \\
& \text{os } \sigma'\text{s are the Pauli matrices}), \\
\alpha \text{ - matrices:} & \alpha^i = \gamma^0\gamma^i,\ a = 1, 2, \\
\text{Conjugate spinor:} & \bar{\psi} = \psi^\dagger\gamma^0.
\end{array} \tag{A.1}$$

B Classical equations in the case of a y-dependent electrostatic field

We consider here a massless particle of charge $q = 1$ in the presence of an electrostatic field $\mathbf{E} = (0, -V'(y))$ derived from the 3-potential $A = (V(y), 0, 0)$ which depends only on the space coordinate y. The equations are given by (2.5), with $m = \psi_5 = 0$ and the partial gauge fixing $\chi = 0$. We restrict ourselves on solutions with the spin variables $\psi^\mu = 0$. With the choice of the worldline parametrization[11] $\lambda = t$ ($t = x^0$), the second of Eq. (2.5) then yields the constraint

$$\dot{x}^2 + \dot{y}^2 = 1, \tag{B.1}$$

i.e., the velocity is that of light. The first of Eq. (2.5) for $\mu = 0$ yields the conservation of total energy ω: $\dot{\omega} = 0$, where

$$\omega = \frac{1}{e(t)} + V(y(t)).$$

For $\mu = 1, 2$, we get

$$\begin{array}{l}
(\omega - V(y))\dot{x} - (\omega - V(\bar{y}))\dot{\bar{x}} = 0, \\
(\omega - V(y))\ddot{y} + (1 - (\dot{y})^2)V'(y) = 0.
\end{array} \tag{B.2}$$

The first of these equations has been obtained by integrating the corresponding second order equation thanks to energy conservation and to the x-independence of the potential, with

[11] We use the notation $x^0 = t$, $x^1 = x$, $x^2 = y$ for the space-time coordinates.

$\bar{y} = y(\bar{t})$ and $\dot{\bar{x}} = \dot{x}(\bar{t})$ as initial values at some initial time $\bar{t}$.

Solutions of the equations of motion (B.2) are uniquely determined by giving 3 boundary conditions, which may be the values of $\bar{y}$, $\dot{\bar{x}}$ and $\bar{x} = x(\bar{t})$, assuming the validity of (B.1) at $\bar{t}$.

It is worthwhile to note that, in the second equation (B.2), the kinetic energy factor $\omega_{\rm kin}(y) = \omega - V(y))$, which can be positive or negative depending on the position y, plays the role of an inertia coefficient [13]. In particular, the sign of the y-component of the acceleration will depend on the sign of $\omega_{\rm kin}(y)$. We may be consider this as a "classical Klein phenomenon".

References

1. O. Klein, Die Reflexion von Elektronen an einem Potentialsprung nach der relativistischen Dynamik von Dirac. Zeitschrift für Physik **53**, 157 (1929)
2. A. Calogeracos, N. Dombey, History and Physics of the Klein Paradox. Contemp. Phys. **40**, 313–321 (1999)
3. N. Stander, B. Huard, D. Goldhaber-Gordon, Evidence for Klein Tunneling in Graphene p-n Junctions. Phys. Rev. Lett. **102**, 026807 (2009)
4. D. Dragoman, Evidence against Klein Paradox in graphene. Phys. Scr. **79**, 015003 (2008)
5. M.I. Katsnelson, K.S. Novoselov, A.K. Geim, Chiral tunnelling and the Klein paradox in graphene. Nat. Phys. **2**, 620–625 (2006)
6. F. Sauter, Über das Verhalten eines Elektrons im homogenen elektrischen Feld nach der relativistischen Theorie Diracs. Zeitschrift für Physik **69**, 742–764 (1931)
7. F. Hund, Materieerzeugung im Anschaulichen und im Gequantelten Wellenbild der Materie. Zeitschrift für Physik **117**, 1–17 (1941)
8. A.I. Nikishov, Pair production by a constant external field. Zh. Eksp. Teor. Fiz. **57**, 1210–1216 (1969)
9. A.I. Nikishov, Pair production by a constant external field. Sov. Phys. JETP **30**, 660 (1970)
10. A.I. Nikishov, Barrier scattering in field theory removal of klein paradox. Nucl. Phys. B **21**, 346–358 (1970)
11. A. Hansen, F. Ravndal, Klein's paradox and its resolution. Phys. Scr. **23**, 1036–1042 (1981)
12. C.W.J. Beenakker, Colloquium: Andreev reflection and Klein tunneling in graphene. Rev. Mod. Phys. **80**, 1337–1354 (2008)
13. I. Morales, B. Neves, Z. Oporto, O. Piguet, Behaviour of charged spinning massless particles. Symmetry **10**(1), 2 (2017)
14. A.H.Castro Neto, F. Guinea, N.M.R. Peres, K.S. Novoselov, A.K. Geim, The electronic properties of graphene. Rev. Mod. Phys. **81**, 109–162 (2009)
15. A.F. Young, P. Kim, Quantum interference and Klein tunnelling in graphene heterojunctions. Nat. Phys. **5**, 222 (2009)
16. V.V. Cheianov, V.I. Fal'ko, Selective transmission of Dirac electrons and ballistic magnetoresistance of n–p junctions in graphene. Phys. Rev. B **74**(4), 041403(R) (2006)
17. T. Tudorovskiy, K.J.A. Reijnders, M.I. Katsnelson, Chiral tunneling in single and bilayer graphene. Phys. Scr. **T146**, 014010 (2012)
18. K.J.A. Reijnders, T. Tudorovskiy, M.I. Katsnelson, Semiclassical theory of potential scattering for massless Dirac fermions. Ann. Phys. (NY) **333**, 155 (2013)
19. V. Kleptsyn, A. Okunev, I. Schurov, D. Zubov, M.I. Katsnelson, Chiral tunneling through generic one-dimensional potential barriers in bilayer graphene. Phys. Rev. B **92**, 165407 (2015)
20. Y. Zhang, Y.-W. Tan, H.L. Stormer, P. Kim, Experimental observation of the quantum hall effect and and Berry's phase in graphene. Nature **438**, 201–204 (2005)
21. K.S. Novoselov, A.K. Geim, S.V. Morozov, D. Jiang, M.I. Katsnelson, I.V. Grigorieva, S.V. Dubonos, A.A. Firsov, Two-dimensional gas of massless Dirac fermions in graphene. Nature **438**, 197 (2005)
22. J.M. Fonseca, W.A. Moura-Melo, A.R. Pereira, Scattering of charge carriers in graphene induced by topological defects. Phys. Lett. A **374**, 4359–4363 (2010)
23. R. Logemann, K.J.A. Reijnders, T. Tudorovskiy, M.I. Katsnelson, Shengjun Yuan, Modeling Klein tunneling and caustics of electron waves in graphene. Phys. Rev. B **91**, 045420 (2015)
24. K.J.A. Reijnders, M.I. Katsnelson, Symmetry breaking and (pseudo)spin polarization in Veselago lenses for massless Dirac fermions. Phys. Rev. B **95**, 115310 (2017)
25. K.J.A. Reijnders, M.I. Katsnelson, Diffraction catastrophes and semiclassical quantum mechanics for Veselago lensing in graphene. Phys. Rev. B **96**, 045305 (2017)
26. K.J.A. Reijnders, D.S. Minenkov, M.I. Katsnelson, S.Yu. Dobrokhotov, Electronic optics in graphene in the semiclassical approximation. Ann. Phys. (NY) **397**, 65 (2018)
27. P. Hosur, X. Qi, Recent developments in transport phenomena in Weyl semimetals. Comptes Rendus Physique **14**(9), 857–870 (2013). (Topological insulators/Isolants topologiques)
28. H.-Z. Lu, S.-Q. Shen, Quantum transport in topological semimetals under magnetic fields. Front. Phys. **12**(3), 127–201 (2017)
29. A. Guevara, P. Pais, J. Zanelli, Dynamical contents of unconventional supersymmetry. JHEP **08**, 085 (2016)
30. P.D. Alvarez, P. Pais, E. Rodriguez, P. Salgado-Rebolledo, J. Zanelli, Supersymmetric 3D model for gravity with $SU(2)$ gauge symmetry, mass generation and effective cosmological constant. Class. Quantum Gravity **32**(17), 175014 (2015)
31. S. Capozziello, R. Pincak, E.N. Saridakis, Constructing superconductors by graphene Chern–Simons wormholes. Ann. Phys. **390**, 303–333 (2018)
32. A. Iorio, G. Lambiase, Quantum field theory in curved graphene spacetimes, Lobachevsky geometry, Weyl symmetry, Hawking effect, and all that. Phys. Rev. D **90**(2), 025006 (2014)
33. A. Iorio, Graphene and black holes: novel materials to reach the unreachable. Front. Mater. **1**, 36 (2015)
34. A. Mesaros, D. Sadri, J. Zaanen, Parallel transport of electrons in graphene parallels gravity. Phys. Rev. B **82**, 073405 (2010)
35. A. Sepehri, R. Pincak, G.J. Olmo, M-theory, graphene-branes and superconducting wormholes. Int. J. Geom. Methods Mod. Phys. **14**(11), 1750167 (2017)
36. A. Iorio, P. Pais, (Anti-)de Sitter, Poincaré, super symmetries, and the two Dirac points of graphene. Ann. Phys. **398**, 265–286 (2018)
37. P.E. Allain, J.-N. Fuchs, Klein tunneling in graphene: optics with massless electrons. Eur. Phys. J. B **83**, 301–317 (2011)
38. A.J. Hanson, T. Regge, The relativistic spherical top. Ann. Phys. **87**, 498–566 (1974)
39. M. Chaichian, R. Gonzalez Felipe, D. Louis Martinez, Anyon in external electromagnetic field: Hamiltonian and Lagrangian formulations. Phys. Rev. Lett. **71**, 3405–3408 (1993). (Erratum: Phys. Rev. Lett., vol. 73, p. 2009, 1994)
40. S. Ghosh, Spinning particles in (2+1)-dimensions. Phys. Lett. B **338**, 235–240 (1994). (Erratum: Phys. Lett., vol. B347, p. 468, 1995)
41. N. Dombey, A. Calogeracos, Seventy years of the Klein Paradox. Phys. Rep. **315**, 41–58 (1999)
42. B. Thaller, *The Dirac Equation* (Cambridge University Press, Cambridge, 1992)
43. M.I. Katsnelson, *Graphene in Two Dimensions* (Cambridge University Press, Cambridge, 2012)

44. A. Calogeracos, N. Dombey, K. Imagawa, Spontaneous fermion production by a supercritical potential well. Phys. Atom. Nucl. **5**, 1275 (1996)
45. P. Krekora, Q. Su, R. Grobe, Klein paradox with spin-resolved electrons and positrons. Phys. Rev. A **72**, 064103 (2005)
46. O.M. Del Cima, E.S. Miranda, Electron-polaron-electron-polaron bound states in mass-gap graphene-like planar quantum electrodynamics: s-wave bipolarons. Eur. Phys. J. B **91**, 212 (2018)
47. Wolfram Research, Inc., Mathematica, Champaign, IL
48. A.P. Balachandran, P. Salomonson, B.-S. Skagerstam, J.-O. Winnberg, Classical description of particle interacting with non-abelian gauge field. Phys. Rev. D **15**, 2308–2317 (1977)
49. L. Brink, S. Deser, B. Zumino, P. Di Vecchia, P.S. Howe, Local supersymmetry for spinning particles. Phys. Lett. B **64**, 435 (1976). (Erratum: Phys. Lett. 68B, p. 488, 1977)
50. V. Ya Fainberg, A.V. Marshakov, Local supersymmetry and dirac particle propagator as a path integral. Nucl. Phys. B **306**, 659–676 (1988)
51. P.A.M. Dirac, *Lectures on Quantum Mechanics* (Dover, New York, 2001)
52. M. Henneaux, C. Teitelboim, *Quantization of Gauge Systems* (Princeton University Press, Princeton, 1992)
53. K. Sundermeyer, *Constrained Dynamics with Application to Yang-Mills Theory, General Relativity, Classical Spin, Dual String Model*, vol. 169 (Springer, Berlin, 1982)
54. D.M. Gitman, I.V. Tyutin, *Quantization of Fields with Constraints. Springer Series in Nuclear and Particle Physics* (Springer, Berlin, 1990)
55. A. Das, *Lectures on Quantum Field Theory* (World Scientific, Singapore, 2008)